Journal of Industrial and Engineering Chemistry 79 (2019) 194–203

Contents lists available at ScienceDirect

Journal of Industrial and Engineering Chemistry

journal homepage: www.elsevier.com/locate/jiec

Investigating the solubility of petroleum asphaltene in ionic liquids and their interaction using COSMO-RS

Zeeshan Rashid[a,b], Cecilia Devi Wilfred[a,c], Regupathi Iyyaswami[e], Arunagiri Appusamy[d], Murugesan Thanabalan[a,b,*]

[a] Centre of Research in Ionic Liquids, Universiti Teknologi PETRONAS, Perak, Malaysia
[b] Department of Chemical Engineering, Universiti Teknologi PETRONAS, Perak, Malaysia
[c] Department of Fundamental and Applied Sciences, Universiti Teknologi PETRONAS, Perak, Malaysia
[d] Department of Chemical Engineering, National Institute of Technology, Trichy, 620015, India
[e] Department of Chemical Engineering, National Institute of Technology Karnataka, Surathkal 575025, India

ARTICLE INFO

Article history:
Received 3 September 2018
Received in revised form 7 May 2019
Accepted 18 June 2019
Available online 27 June 2019

Keywords:
COSMO-RS
Ionic Liquids: Asphaltene
Dispersion

ABSTRACT

Dispersion of asphaltene in crude oil using ionic liquids (ILs) is being considered as a viable solution, in extraction and transportation processes. In this work, the interplay between asphaltene and ILs has been studied systematically to understand the effect of structural variation of ILs on asphaltene solubility. The activity coefficient of the total of 1517 ILs with different combinations of cation and anion of ILs for representative asphaltene molecule (asphaltene) was estimated via COSMO-RS (Conductor-like Screening Model for Real Solvents). COSMO_RS predictions were validated using experimental data on asphaltene solubility. Among the studied ILs, asphaltene showed high solubility in imidazolium-based ILs with hydrophobic anions. The present approach paved a way forward to rationally understand the impact of structural variation of ILs on their interaction with asphaltene molecule and to design new ILs for the dispersion and stabilization of asphaltene.

Introduction

The supply of conventional light oil has been decreasing at an alarming rate, as they are the first choice for oil refineries and various petrochemical manufacturing industries [1,2]. Consequently, oil producers are using heavy crude oil reservoirs and offshore fields [3]. There is no defined terminology for asphaltene; it is defined only by SARA analysis which is based on the crude oil's major components; Saturates, Aromatics, Resin and Asphaltene (SARA) [4]. Heavy components in crude oil such as asphaltene are problematic in terms of processing and economics in the energy sector [5]. Heavy crude oils can only be extracted from wells either by injecting gases such as steam and carbon dioxide or by the addition of diluents to alter their rheological properties [2,6]. However, these additives can trigger the asphaltene aggregation and responsible for the precipitation of asphaltene [7,8]. Asphaltene tends to precipitate during transportation, plugging the downstream pressure vessels and blocking the reservoir porosity [9]. Therefore, making the oil extraction and cost-effective refining process while using asphaltenic crude oil as feedstock is the critical challenge in the global oil and gas sector.

Stability of asphaltene in oil can be enhanced by the use of a variety of organic solvents with distinctive solubility parameters [6,9,10]. The aromatic solvents blended with toluene and xylene can dissolve asphaltic deposits and have been used to cast off asphaltene deposits from oil pipelines, but those volatile organic solvents (VOC) are harmful to the environment [11–13]. In addition, the mixing of alternative solvents which include amine and alkyl benzene sulfonic acid has significantly improved the asphaltene precipitation inhibition via acid-base interaction [14]. Reported literature confirmed that the direct adsorption of amphiphile at the surface of asphaltene and get attached to the asphaltene molecules and form large conjugated systems [15]. Therefore, the asphaltene-amphiphile interaction is the electrophilic addition reaction which makes the irreversible bond between them [14]. However, they associate together and precipitate in non polar media. As a result, the solubility of asphaltene diminishes due to the aggregation of the asphaltene-amphiphile complex [16].

Recently, another class of solvents called Ionic liquids (ILs) has been used for solving asphaltene aggregation problem due to their

* Corresponding author at: Department of Chemical Engineering, Universiti Teknologi PETRONAS, Perak, Malaysia.
E-mail address: murugesan@utp.edu.my (M. Thanabalan).

https://doi.org/10.1016/j.jiec.2019.06.034
1226-086X/

many benefits, which include the improved solubility, low volatility, targeted rheological properties and extensive temperature range for liquid phase [17–19]. In addition, ILs may be finely tuned through the careful selection of cations and anions to adjust the targeted properties for asphaltene stabilization [20–22]. Therefore, efforts have been devoted to recognize the mechanism of asphaltene and its interaction with ILs to develop new ILs for the solubility of asphaltene [16,23,24]. The details of the ILs used, and their factors influencing the asphaltene aggregation and dispersion phenomena are compiled in Table 1.

The asphaltene solubility studies using ILs suggested that cations tend to get attached at heteroatoms of asphaltene molecule due to the strong electrostatic interactions with asphaltene's polar moiety, while anions mainly interact with asphaltene core via hydrogen bonding, $\pi-\pi$ interaction and the shielding effect of anions [19,25]. However, the impact of structural variations of ILs on asphaltene-IL interaction, the chemistry behind the solubility of asphaltene and the stability of asphaltene in ILs have not been systematically explored.

Nevertheless, there is a significant scope to either design or choose targeted ILs with better performance as asphaltene precipitation inhibitor with defined physiochemical characteristics [25–28]. Therefore, the ILs must have a targeted dispersive ability for the asphaltene molecules. Experimental testing is a time consuming and impractical method to investigate and identify the ILs with high dispersive potential for the asphaltene whereas computer simulation tools (COSMO-RS, Conductor-like Screening Mode for Real Solvents) [29–31] provides an alternate yet the practical route.

COSMO-RS is a well-articulated thermodynamic version that uses the atomic configuration of compounds of interest rather than their experimental data [32–34]. This tool has been used to predict the thermodynamic characteristics and phase envelops of ILs, e.g., enthalpy of vaporization[35,36], gas absorption studies [37,38], limiting dilution activity coefficient of individual compounds [39,40], phase equilibria of organic liquids [38] and dispersing potential of ILs for drugs [41,42], etc. Even though, COSMO-RS has been proved to help in designing solvents in desulfurization [43], denitrification [44], alkane/aromatic and aromatic/aromatic separation [45], drug delivery studies [41], separation of aromatics from model oil [46] and quantification of drug similarity [47] applications. The dispersive potential of ILs for asphaltene with the help of COSMO-RS is yet to be investigated.

The purpose of this work is to examine the interaction between the different kind of ILs (halide, protic, aprotic, hydrophilic and hydrophobic) and asphaltene molecule to investigate the impact of structural variations of the ILs on the IL-asphaltene complex formation. Therefore, a combination of 37 cations and 41 anions with a total of 1517 ILs has been considered for the present study. Quantum calculations and thermodynamic model (COSMO-RS) were used to do a micro-level investigation on the interaction between these ILs and asphaltene molecules. The development of a model compound for asphaltene has been reported in our previous study [25]. The terminology and abbreviations for the cations and anions of the studied ILs are shown in Table S1 and Table S2 respectively. This study will be helpful to understand the impact of structural variations of ILs on their interplay with asphaltene molecule and to design new ILs for the solubility and stabilization of asphaltene.

Methodology

Chemicals

Asphaltene used in the present study was extracted from RATAWI crude oil, via ASTM D6560. Analytical grade toluene (purity >99.8%) and heptane (purity > 99%) were purchased from

Table 1
ILs used for aggregation inhibition studies of petroleum asphaltene.

Sr #	ILs	Study	Findings	Remarks
1	1-propyl boronic acid-3-hexadexylimidazlium Bromide $[B(OH)_2C_3C_{16}im]$ [Br] [16]	Petroleum dispersion studies in polar -nonpolar media.	Asphaltene dispersion is due to; • Electrostatic interaction between boronic acid moiety and asphaltene functional group. • Hydrophobic interaction between the cation side chain and nonpolar media of oil.	IL-asphaltene complex has both electrostatic and non-electrostatic interactions.
2	Dodecylphenolic resin. and Poly (octadecene maleic anhydride) [15].	Interaction study between asphaltene and dispersants.	Asphaltene dispersion is due to; • Electrostatic interaction between ILs cations head and asphaltene molecule • Hydrophobic interaction between the cation alkyl chain of the ILs and oil.	IL-asphaltene complex has both electrostatic and non-electrostatic interactions.
3	1-methyl-1H-imidazol-3-ium-2-carboxybenzoate [24]	Dispersion of petroleum asphaltene in IL. Molecular modeling to study the interaction between asphaltene and IL.	Asphaltene dispersion is due to; • Interaction of IL-asphaltene complex is through electron donation from the anion of IL to the electron acceptor site of the asphaltene. • These interactions are controlled by CH- π bond in IL-asphaltene complex.	Charge transfer and $\pi-\pi$ interaction held responsible for asphaltene dispersion. Asphaltene-ILs complex form via $\pi-\pi$ interaction between cation and asphaltene, charge transfer and hydrogen bonding.
4	(3-(2-carboxybenzoyl)-1-methyl-1H-imidazol-3-ium chloride [23]	Aggregation inhibition of petroleum asphaltene	Asphaltene dispersion is due to; • Acidic moiety in IL prevents the asphaltene deposition with the help of hydrogen bonding and electrostatic interaction.	The aromatic moiety, through $\pi-\pi$ and dipole interactions, may be amongst the prevailing contributors to asphaltene association.
5	*n*-alkylpyridinium chloride ([Cnpy] [Cl]), *n*-alkyl isoquinolium chloride ($[C_niq][Cl]$), *n*-alkylpyridinium tetrafluoroborate ($[C_npy][BF_4]$) and *n*-alkylpyridinium hexafluorophosphate ($[PF_6]$)n = 4–12 [14]	Asphaltene precipitation inhibition from high pressure, CO_2 injected reservoir oils by IL.	Asphaltene dispersion is due to; • Non polar cation and anion with high charge density can prevent asphaltene precipitation. • These cations of ILs cannot have a stable bond with asphaltene and form complexes because of a low density of the cation.	Steric stabilization of cation tail is necessary to avoid asphaltene micelles from aggregating. The acid-base connections between the cationic heads of the ILs and asphaltene have an impact on their capacities to keep asphaltene precipitated from repository oil.

Merck. The ILs, 1-butyl-3-methyl-imidazolium Bromide [BMIM][Br] (purity 98.5%), 1-butyl-3-methyl-imidazolium bis(trifluoromethylsulfonyl)imide [BMIM][NTf_2] (purity 98.0%), 1-butylpyridinium bis(trifluoromethylsulfonyl)imide [BPy][NTf_2] (purity 99%) and 1-butyl-3-methyl-imidazolium tetrafluoroborate [BMIM][BF_4] (purity 97%) were purchased from Sigma Aldrich. All the chemicals were used without further purification.

Computational procedures

It is not always practically possible to carry out quantum calculations for petroleum asphaltene with an almost infinite range of atoms. A viable and suitable approach for asphaltene modeling is to select the representative part of the asphaltene that is as small as to permit quantum chemical calculations while on the other hand, it should be large enough to display chemical characteristic of the molecule. The motivation for modifying model asphaltene compound was taken from the literature [48–50]. Perylene based compound having the hydrophobic part and an acidic moiety at its surroundings has already been proven to possess the similar properties of asphaltene [25,51,52]. Perylene based model compound was modified and developed for screening of ILs for asphaltene solubility study [25]. In the present study, we utilized the developed model compound to investigate the binary interaction of the IL with asphaltene for solubility studies. Fig. 1 shows the structure of a model asphaltene compound, abbreviated as "asphaltene." The red color balls represent the oxygen atoms, blue color balls show nitrogen atoms, green color balls represent carbon atoms, and white color balls show hydrogen atoms. The molecular simulation was completed in following the multistep route as shown in Fig. 2. A COSMO polarization calculation of the molecular surface charge densities (σ) of the model compound was made by TmoleX [53] (version 4.2.1) software at the density functional theory with empirical dispersion correction (DFT-disp) level using B3LYP (DFT-D3 BJ-damping) functional with TZVP (triple zeta valence potential) basis set [53]. COSMO files of the anions and cations used in this study have been taken from the database of BP-TZVP-IL (COMOlogic GmbH & Co. KG, Leverkusen, Germany). All the calculations for predicting the solubility of asphaltene molecule in the ILs have been achieved by using of COSMOthermX (version C30-1601, COMOlogic GmbH& Co.KG).

Unlike conventional solvents, ILs are described as a combination of ions (positive and negative) or both as individual species [25,26,54]. ILs are considered as charged neutral species which are used for predicting the chemical potential of various species in ILs [25,55–57]. In this study, the charge-neutral combination is implemented to model asphaltene and the ILs. Thus, the equimolar approach has been used in the investigation that is the reason why the ILs are treated as a single compound. The ternary system (asphaltene, cation, and anion) was converted into binary mixtures (asphaltene and IL) to investigate the interaction between asphaltene and IL. The information on the calculation procedures for estimating the thermodynamic properties of solutes in ILs via COSMO-RS can be found elsewhere [27,44,57,58].

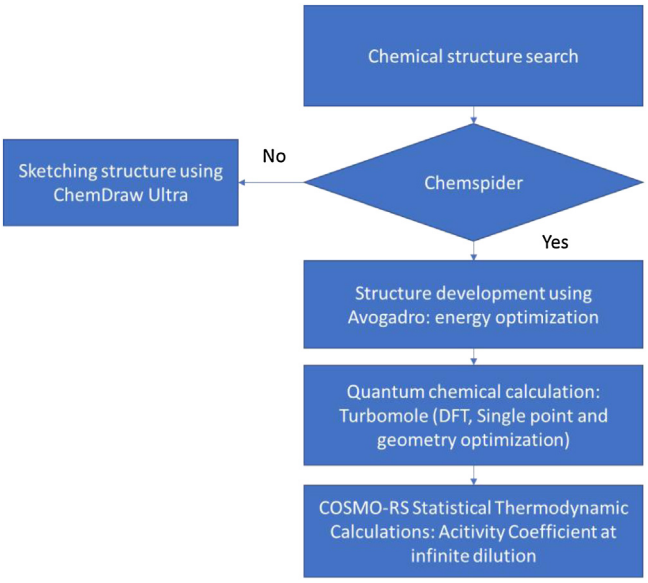

Fig. 2. Molecular simulation scheme for thermodynamic calculations [25].

Activity coefficient at infinite dilution

Activity coefficient (AC) is the thermodynamic variable used to measure the chemical potential for the solute both within the solvent as well as in the pure state [58–60]. At infinite dilution, the solute is surrounded only by the solvent molecules, and the solute-solute interplay is negligible while solute–solvent interaction dominates which is known as infinite dilution activity coefficient ($\gamma\infty$) [55,58,61,62]. It is used to estimate the solubility magnitude for the solvents such as conventional volatile organic solvents as well as ILs [63–65]. Kahlen et al. [66] and Ana Cases et al. [67] carried out activity coefficient prediction using COSMO-RS to evaluate the solubility of complex polymer compounds (lignin and cellulose) in ILs. Moreover, Girma et al. [68] investigated the interaction between DNA nucleotides and IL with the help of predicted AC using COSMO-RS. Since asphaltene is considered as macromolecules [69–71], a similar procedure can be considered to predict the solubility of asphaltene in ILs. The measurable description of asphaltene solubility in ILs can be expressed through the following simplified equation [66].

$$x_i^L = \frac{1}{\gamma_i^L}\exp\left[\frac{\Delta h_{m,i}}{RT}\left(\frac{T}{T_i^m}-1\right)\right] \quad (1)$$

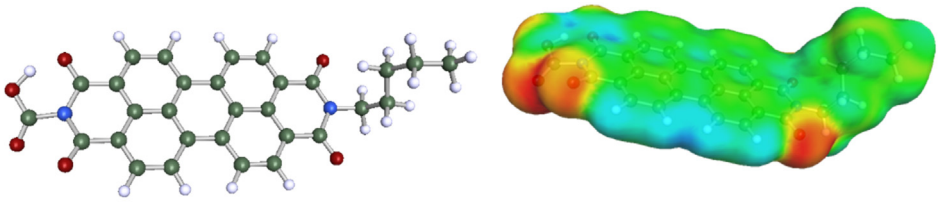

(a) (b)

Fig. 1. Model asphaltene compound (asphaltene) (a) 2 D structure of asphaltene; oxygen atom (red color), nitrogen atom (blue color), carbon atom (green color) and hydrogen atoms (white color) (b) 3 D structure of asphaltene [25]. (For interpretation of the references to colour in this figure legend, the reader is referred to the web version of this article.)

Where, x_i^L is the mole fraction of the dissolved component *i* in a saturated solution in equilibrium with the solid '*i*', $\Delta h_{m,i}$ and T_i^m denote the enthalpy of melting and the melting temperature of component i, respectively. According to Eq. (1), the exponential term remain constant as the calculation has to be done at constant temperature and fixed system (solute–solvent complex), Therefore, the inverse of activity coefficient at infinite dilution can qualitatively represent the dissolvability of the asphaltene within the ILs which means, the decrease in activity coefficient of ILs for asphaltene results in better solubility in ILs [44,57,72].

Excess enthalpy

The excess enthalpy of the asphaltene-IL complex permits the assessment of the interaction by every species and their contribution. It can also be used to deduce the strength of asphaltene-ILs interaction inside the binary mixture [57,67]. The calculation of excess enthalpies of the mixture by COSMO-RS has been effectively carried out to analyze the thermodynamic behavior of alkyl esters with dibromoalkanes [73], desulfurization [58], denitrification [44], aromatic extraction [27] and interaction study between DNA nucleotides and biocompatible Ionic liquids [68]. According to the COSMO-RS model, the excess enthalpy of the mixture (H_m^E) is the sum of hydrogen bond interaction (H^E_{HB}), Van der Waals interaction (H_{vdW}^E), and electrostatic/misfit interaction (H_{MF}^E) energy as shown in the following equation: [67,68]

$$H^E_m = H^E_{MF} + H^E_{HB} + H^E_{vdW} \quad (2)$$

Consequently, the approach can be used to analyze the data on the enthalpy of the mixture in terms of the exclusive intermolecular interactions among the model asphaltene compound with ILs.

Results and discussion

Validation of COSMO-RS results

Since no information on the experimental data concerning the activity coefficient of asphaltene in ILs is available, the COSMO-RS predictions concerning the solubility of asphaltene molecule in ILs have been validated by dispersion index (DI%) values of the four ILs ([BMIM] [Br], [BMIM][NTf_2], [BPy][NTf_2] and [BMIM][NTf_2] which were experimentally determined [74]. Since these ILs are liquids at room temperature (RTILs), the solubility measurements of asphaltene in ILs were performed at 298 K.

For the experimentation, 800 ppm of asphaltene solution was prepared in toluene. The 1 mMol of targeted IL was added to the sample solution followed by the addition of heptane with toluene to heptane ratio of 1:2. The mixture was stirred at 298 K at 400 rpm for 1 h. The samples were centrifuged at 4000 rpm for 20 min. and filtered using a 0.22 μ nylon filter. The calibration curve was established by using a series of asphaltene solution in toluene ranges from 100 to 1000 ppm to measure the concentration of asphaltene in the hydrocarbon mixture [23,74]. The concentration was measured using UV–vis spectroscopy with the range of 200–800 nm. The asphaltene solution gave the peak at 346 nm which agrees well the literature[16,23,24]. The predicted and experimental data of solubility of asphaltene in the studied ILs is shown in Fig. 3. The experimental values for the selected ILs are lower than calculated values which is similar to the solute prediction by other techniques [44,58]. Moreover, the trend of the inverse of activity coefficients of selected ILs for asphaltene resembles with the experimental values of asphaltene solubility which agrees with the theory that lower values of activity coefficient bring better asphaltene solubility.

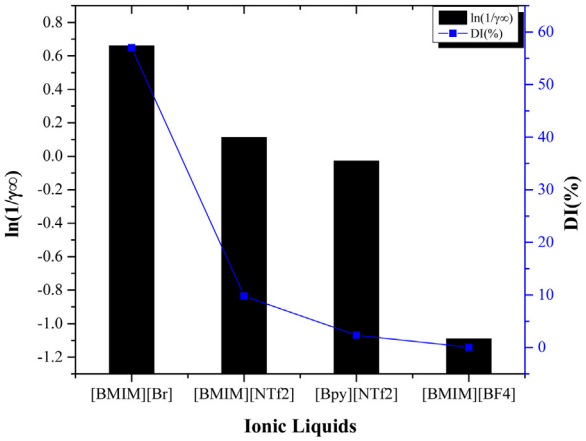

Fig. 3. Predicted and experimental solubility of asphaltene in [BMIM][Br], [BMIM][NTf_2], [BPy][NTf_2], [BMIM][BF_4].

The structural effect of ILs on activity coefficient at infinite dilution

Based on COSMO-RS calculations, the predicted activity coefficient data at infinite dilution of ILs for asphaltene are shown in Fig. S1. The results show that the activity coefficient depends on the combination of cation and anion of the ILs, i.e., cation head and the nature of anion; e.g., the activity coefficient values of [Ac] based ILs for asphaltene are between −10.1 to 8.5 whereas the same for [PF_6] based ILs are in the range of −3.0 to 0.5. The impact of the anion is more pronounced than that of the cation. Therefore, a thorough examination of the effects of structural variation of ILs namely cation head group, length of the alkyl chain of cation and anion, type of anion and functional group of anions on activity coefficient is needed.

The impact of cation nature on asphaltene dispersion

The IL containing various cation head families, i.e., imidazolium, pyridinium, piperidinium, pyrrolidinium, and quinolinium are used for present investigation. Impact of cation family on asphaltene dispersion are demonstrated in Fig. 4. Cation family remarkably affects the activity coefficient of IL for asphaltene particle, for instance, $[C_6C_1im]^+$, $[C_6C_1py]^+$, $[C_6C_1pyr]^+$, $[C_6q]^+$ and $[C_6C_1pip]^+$ have same alkyl tail but different cation heads. Their estimated activity coefficient values are significantly different. The order of activity coefficient of ILs for asphaltene are as follows: $[G]^+$

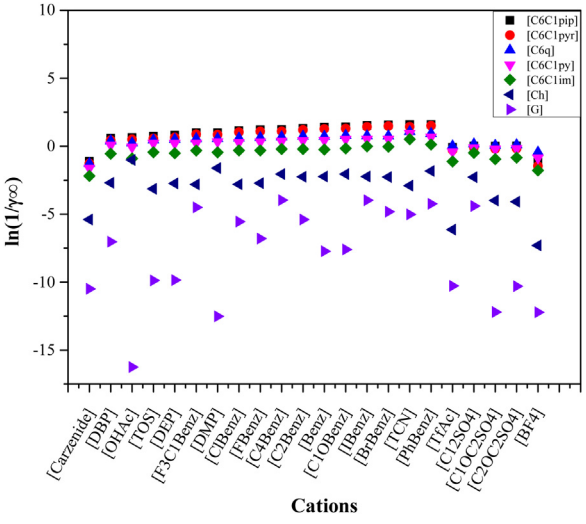

Fig. 4. Activity coefficient at infinite dilution at 298.15 K of ILs for asphaltene.

> $[Ch]^+ > [C_6C_1Py]^+ > [C_6q]^+ > [C_6C_1Pyr]^+ > [C_6C_1pip]^+ > [C_6C_1im]^+$.

The trends of asphaltene solubility in the present studied ILs with various cation families is represented in Fig. 4, and the data on the hydrogen bond interaction, Van der Waals interaction and electrostatic/misfit interaction energies are shown in Table 2 and 3.

In Fig. 5, the sigma profile peaks for $[C_6C_1im]^+$, $[C_6C_1pyrr]^+$, $[C_6C_1pip]^+$, $[C_6C_1py]^+$, $[C_6q]^+$ are situated in the non polar region of $\sigma = -0.01 e/A^2$ to $\sigma = 0.01 e/A^2$ and the sequence of peak area are as follows: $[C_6C_1pip]^+ < [C_6C_1Pyr]^+ < [C_6q]^+ < [C_6C_1Py]^+ < [C_6C_1im]^+$ while the peaks for $[G]^+$ and $[Ch]^+$ are situated in polar region, $\sigma = -0.018$ e/A^2 and -0.009 e/A^2 respectively. Subsequently, non polarity of these cations increases as follow: $[C_6C_1pip]^+ > [C_6C_1Pyr]^+ > [C_6q]^+ > [C_6C_1im]^+ > [C_6C_1Py]^+ > [G]^+ \approx [Ch]^+$. The trend for nonpolarity is generally similar to that of the activity coefficients of the present studied ILs for asphaltene. Among various factors responsible for the interaction between cation and asphaltene [16,23,25], two factors are of vital importance; (1) hydrogen bonding between cation and heteroatom of asphaltene, (2) interaction with delocalized electron cloud of interacting species [25,75]. The cations containing aromatic ring show less affinity towards asphaltene molecule. It is due to the charge delocalization in aromatic ringed cations which provides steric hindrance towards the polar moiety of asphaltene [55,76]. However, number of heteroatoms in cation head increases the charge sharing ability of cation which in turn enhances the interaction with poly-aromatic molecule [25,56,57,61,77]. It can be concluded that high non-polar cation head family with charge sharing ability brings about lower activity coefficient which implies better interaction between IL and asphaltene molecule. The sigma profile of other studied cations is shown in Fig. S2.

In addition to the sigma profile analysis, the nature of the studied cation can also be seen by their related interaction energy values, i.e., (H^E_{HB}), (H^E_{vdW}), and (H^E_{MF}) of various asphaltene/IL combinations calculated via COSMO-RS, as shown in Fig. 6. The (H^E_{HB}) indicates the hydrogen bond donor capability [55], whereas (H^E_{vdW}) and (H^E_{MF}) values represents the Van der Waals interaction energy and electrostatic/misfit interaction of ILs on the targeted solute, respectively [54,55,57]. The (H^E_{HB}) values of studied cations are listed in Table 2 whereas (H^E_{vdW}) and (H^E_{MF}) values relating to asphaltene/IL interaction are given in Table 3. The present results show that the cations with high polarity have the higher hydrogen bond donor value (Fig. 6) which is due to the absence of delocalized charge on the polar cations which in turn increases the electrostatic strength and compactness of ILs as reported in literature [78]. In addition, Fig. 6 shows that cations with high non polarity have higher Van der Waals and misfit energies and low compactness which resulted in better interaction with asphaltene molecule. It is due to the fact that the solubility of ILs are more dependent on the compactness of ILs rather than on the acidity of the cation [78–80]. Compactness of ILs has an inverse effect on the solubility strength of ILs [79,80]. Less compact ILs have the ability to easily realign their cation and anion to accommodate poly-aromatic molecule [69,78,81]. Similar trend has been reported for the study of desulfurization and denitrification using ILs using the similar computational tool [57,72].

Effect of alkyl chain length. The impact of alkyl chain length of imidazolium cation ($[C_nC_1im]$), where n = 2, 4,6,8,10,12, on the solubility of asphaltene are illustrated in Fig. 7. The magnitude of interaction increases as the number of carbon atoms in the alkyl chain of cation increases and the trend is shown as follows: $[C_2C_1im]^+ < [C_4C_1im]^+ < [C_6C_1im]^+ < [C_8C_1im]^+ < [C_{10}C_1im]^+ < [C_{12}C_1im]^+$. The effects of cation alkyl chain length are similar to those of the other cation family and can be explained in a similar way. The sigma profile peaks of all the studied $[C_nC_1im]$ cations and their areas lie in the range of non polar region, (Fig. S3). It is observed that with the increase in the length of an alkyl chain, non polarity and hydrophobicity of the studied cations increases. Moreover, the peak area of sigma profile, non polarity, and van der Waal energies increase upon increasing the alkyl tail of cation. Consequently, these factors provide significant affinity for asphaltene molecule and the higher dissolvability which can be comprehended by the interaction energies data (Table 2 and 3). The correlation among moment values (H^E_{HB}), (H^E_{vdW}) and (H^E_{MF}) for the present studied ILs is shown in Fig. S4. Molecular size increases as the side chain length of the cation is increased which on the other hand decreases the polarity and charge density of ILs. In addition, ILs containing large nonpolar surface would cause less compactness which provide conducive environment for asphaltene dissolution. Consequently, the solubility of asphaltene in the present studied ILs increases with the increase in the carbon atoms of the cation side chain. Similar inference can de deduced for the present studied pyridinium, pyrrolidinium, quinolinium, piperidinium and ammonium based ILs (Figs. S5–S7 and Tables 2 and 3).

Effect of functional group. Three types of functional groups with three different cation families are chosen to study the effect of the functional group attached to cation on the dispersive ability of the

Table 2
COSMO descriptor HB_doner moment for studied cations.

Cations	HB-don	Cations	HB-don
1-ethyl-3-methyl-imidazolium	1.939	1-(cyanomethyl)-1-methylpiperidinium	4.285
1-butyl-3-methyl-imidazolium	1.917	1-(2-hydroxyethyl)-1-methylpiperidinium	2.822
1-hexyl-3-methyl-imidazolium	1.899	1-ethyl-3-methylpyridinium	0.931
1-octyl-3-methyl-imidazolium	1.927	1-butyl-3-methyl-pyridinium	0.966
1-decyl-3-methyl-imidazolium	1.916	1-hexyl-3-methyl-pyridinium	0.994
1-dodecyl-3-methyl-imidazolium	1.913	1-butylquinolinium	0.725
1-(ethoxymethyl)-3-methyl-imidazolium	2.535	1-hexylquinolinium	0.726
1-(2-hydroxyethyl)-3-methylimidazolium	4.439	1-octylquinolinium	0.721
3-(cyanomethyl)-1-methyl-imidazolium	7.077	Tetramethylammonium	0.377
1-ethyl-1-methyl-pyrrolidinium	0.058	Butyltrimethylammonium	0.258
1-butyl-1-methyl-pyrrolidinium	0.054	Hexyltrimethylammonium	0.233
1-hexyl-1-methyl-pyrrolidinium	0.053	Octyltrimethylammonium	0.225
1-octyl-1-methyl-pyrrolidinium	0.054	Trimethylethylammonium	0.250
1-(ethoxymethyl)-1-methylpyrrolidinium	0.171	decyl-trimethyl-ammonium	0.232
1-(cyanomethyl)-1-methylpyrrolidinium	4.297	tetra-ethylammonium	0.022
1-(2-hydroxyethyl)-1-methylpyrrolidinium	2.766	tetra-*n*-butylammonium	0.019
1-butyl-1-methylpiperidinium	0.078	Choline	3.082
1-hexyl-1-methylpiperidinium	0.076	Guanidinium	23.815
1-(ethoxymethyl)-1-methylpiperidinium	0.267		

Table 3
Misfit, Hydrogen Bonding, and Van der Waals Energies for the capacity of asphaltene in the [NTf_2] based ILs at 298.15 K.

Sr No.	ILs cations	H^E_{MF} (kcal/mol)	H^E_{HB} (kcal/mol)	H^E_{vdW} (kcal/mol)
1	1-ethyl-3-methyl-imidazolium	7.894	−1.201	−19.247
2	1-butyl-3-methyl-imidazolium	7.529	−1.165	−19.487
3	1-hexyl-3-methyl-imidazolium	7.266	−1.132	−19.666
4	1-octyl-3-methyl-imidazolium	7.07	−1.106	−19.809
5	1-decyl-3-methyl-imidazolium	6.914	−1.067	−19.937
6	1-dodecyl-3-methyl-imidazolium	6.788	−1.039	−20.04
7	1-(ethoxymethyl)-3-methyl-imidazolium	7.689	−1.36	−19.308
8	1-(2-hydroxyethyl)-3-methylimidazolium	7.82	−2.489	−18.991
9	3-(cyanomethyl)-1-methyl-imidazolium	8.037	−2.044	−19.077
10	1-ethyl-1-methyl-pyrrolidinium	8.175	−0.684	−19.041
11	1-butyl-1-methyl-pyrrolidinium	7.78	−0.652	−19.295
12	1-hexyl-1-methyl-pyrrolidinium	7.508	−0.624	−19.483
13	1-octyl-1-methyl-pyrrolidinium	7.299	−0.6	−19.64
14	1-(ethoxymethyl)-1-methylpyrrolidinium	7.806	−0.744	−19.215
15	1-(2-hydroxyethyl)-1-methylpyrrolidinium	7.9	−2.287	−18.795
16	1-(cyanomethyl)-1-methylpyrrolidinium	8.124	−1.721	−18.922
17	1-butyl-1-methylpiperidinium	7.694	−0.647	−19.367
18	1-hexyl-1-methylpiperidinium	7.448	−0.619	−19.539
19	1-(ethoxymethyl)-1-methylpiperidinium	7.689	−0.746	−19.31
20	1-(2-hydroxyethyl)-1-methylpiperidinium	7.789	−2.279	−18.911
21	1-(cyanomethyl)-1-methylpiperidinium	8.027	−1.664	−19.047
22	1-ethyl-3-methylpyridinium	7.849	−1.002	−19.4
23	1-butyl-3-methyl-pyridinium	7.53	−0.956	−19.594
24	1-hexyl-3-methyl-pyridinium	7.284	−0.931	−19.76
25	1-butylquinolinium	7.399	−0.878	−19.866
26	1-hexylquinolinium	7.189	−0.853	−19.99
27	1-octylquinolinium	7.036	−0.822	−20.096
28	tetramethylammonium	8.415	−1.058	−18.625
29	trimethylethylammonium	8.272	−0.931	−18.856
30	butyltrimethylammonium	7.811	−0.894	−19.168
31	hexyltrimethylammonium	7.497	−0.848	−19.391
32	octyltrimethylammonium	7.261	−0.813	−19.576
33	decyl-trimethyl-ammonium	7.08	−0.784	−19.719
34	tetra-ethylammonium	7.964	−0.594	−19.276
35	tetra-*n*-butylammonium	7.14	−0.491	−19.887
36	Choline	8.042	−2.457	−18.565
37	Guanidinium	6.962	−4.501	−18.342

studied IL for asphaltene molecule. The functional groups considered are; ether [C_2OC_1], hydroxyl [OHC_2] and cyanide [CNC_1] and their estimated activity coefficients are shown in Fig. 8. The dispersive capacity of the studied ILs for asphaltene decreases with the addition of functional groups (Fig. 8). It is reported that the asphaltene molecule is mostly non polar due to the fused poly-aromatic hydrocarbon rings which induce hydrophobicity in the molecule [25,57]. The addition of functional group shifts the sigma profile of the present studied cations towards the polar region (Fig. S2), which adversely affects the dispersive capacity of the studied ILs for asphaltene molecules. It is due to the induced polarity of cation by a functional group which increases the compactness between cation and anion that hinders the π–π interaction of anion with the aromatic core of asphaltene [82]. The trend agrees well with the investigation of molecular interaction between ILs and heterocyclic nitrogen compounds for denitrogenating and desulfurization studies

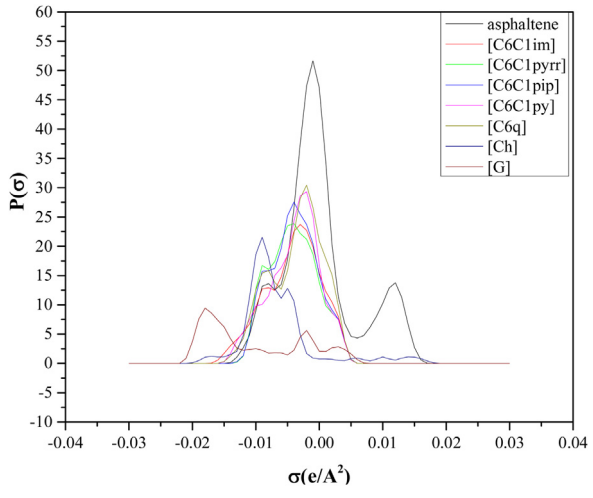

Fig. 5. Sigma profile of asphaltene and seven studied cations.

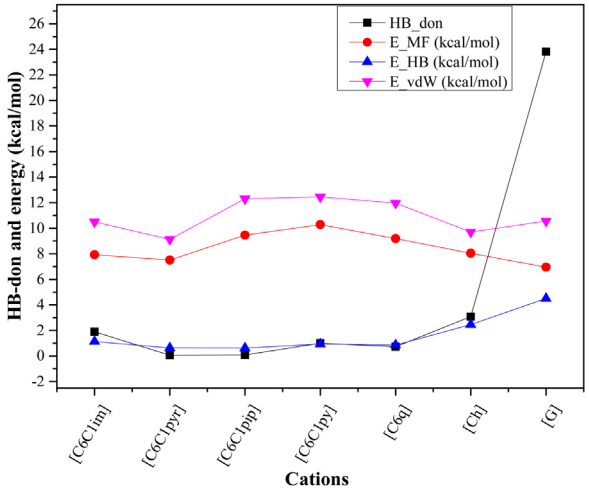

Fig. 6. Relationship between the H^E_{HB} with the HB energy, H^E_{vdW} and H^E_{MF} of seven studied cations.

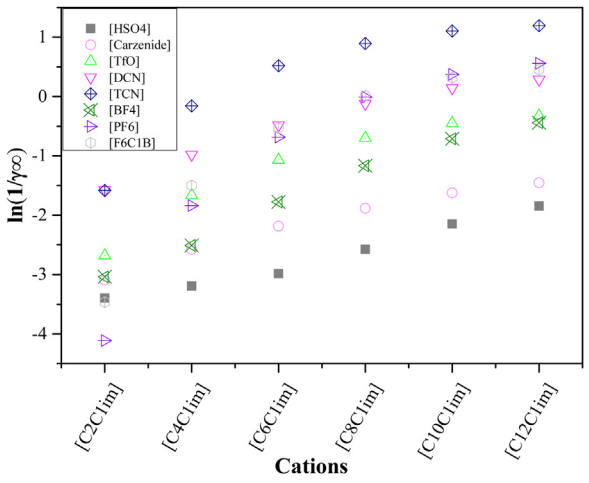

Fig. 7. Activity coefficient values of [$C_nC_1$im] based ILs for asphaltene.

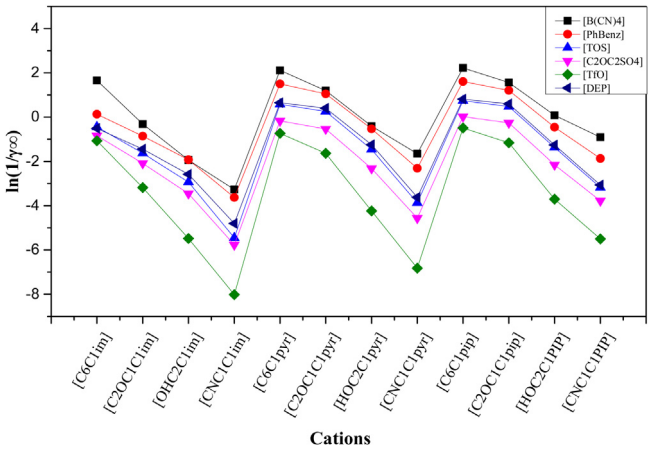

Fig. 8. Capacity data of studied functionalized ILs for asphaltene at 298.5 K.

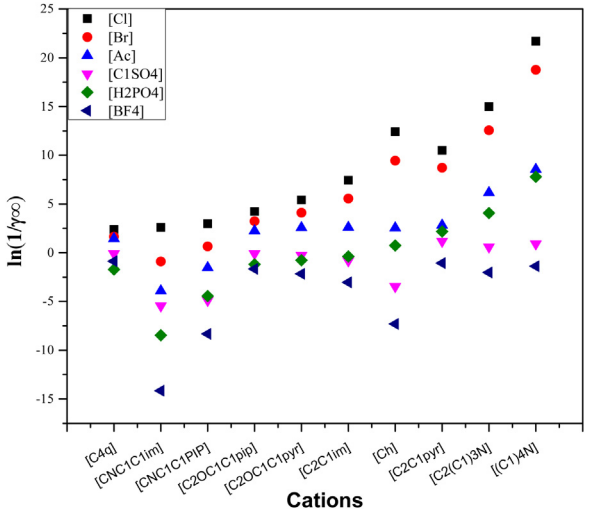

Fig. 9. Activity coefficient values of studied ILs for asphaltene at 298.5 K.

[78,82]. Similar conclusion can be deduced with the help of hydrogen bonding, misfit and van der Waal energies data (Table 3).

Based on the above discussion, it can be concluded that the high nonpolar cations with charge sharing ability, van der Waal dispersive energies, hydrogen bonding ability, and their low

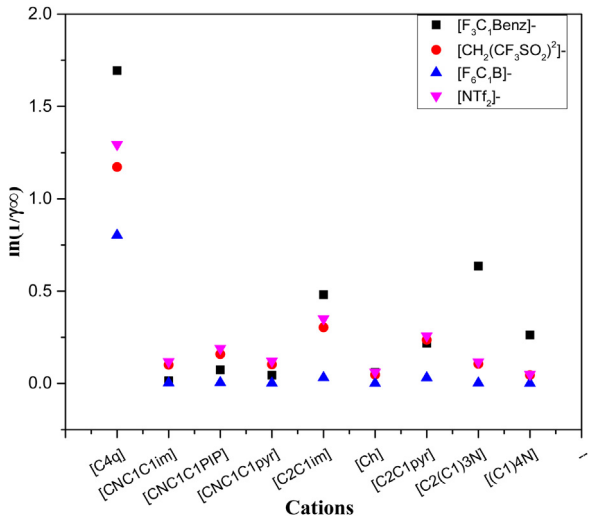

Fig. 10. Activity coefficient value of studied hydrophobic ILs for asphaltene at 298.5 K.

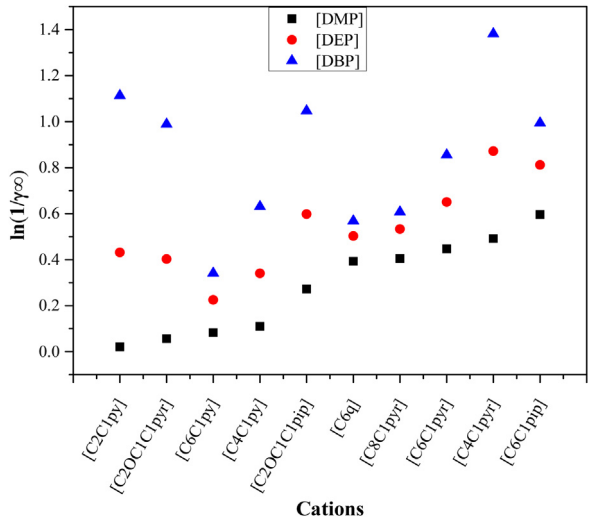

Fig. 11. Activity coefficient values of [DC_nP] based studied ILs for asphaltene at 298.5 K.

compactness enhance the dispersive capability for asphaltene molecule. The proton donating strength of the cation enhances the hydrogen bonding network to the heteroatoms of the asphaltene molecules. Moreover, the loosely compacted ILs provide better mobility of anion to interact with asphaltene.

The effect of anion nature on asphaltene dispersion

The trends of estimated activity coefficients at infinite dilution for asphaltene model compounds in the present studied ILs with different anions are shown in Fig. 9. The interaction capability for asphaltene with the present studied ILs follow the order: $[Cl]^- < [Br]^- < [Ac]^- < [H_2PO_4]^- < [C_1SO_4]^- < [BF_4]^-$. The anions having high dissolution capacity for asphaltene molecule, have high polarity (Fig. S8) where the peak area of the studied anions is in the positive region of $0.01 < \sigma\ (e/A^2) < 0.03$ with peak heights at $[Cl]^-$ (0.019), $[Br]^-$ (0.017), $[Ac]^-$ (0.02), $[C_1SO_4]^-$ (0.015), $[H_2PO_4]^-$ (0.02) and $[BF_4]^-$ (0.011). The magnitude of hydrogen bond acceptor and related energies of anions can also be used to comprehend the polarities of these anions, and these values are given in Tables 2 and 3 respectively. The high polarity of anions is due to the high magnitude of hydrogen bond acceptor and related energies (Fig. S9).

Table 4
COSMO descriptor HB_acceptor for studied anions.

Anions	HB-acc	Anions	HB-acc
[Cl]	36.628	[FBenz]	31.588
[Br]	29.644	[ClBenz]	30.751
[I]	18.835	[BrBenz]	30.916
[Ac]	38.928	[IBenz]	30.686
[OHAc]	31.765	[C_1OBenz]	34.082
[TfAc]	20.208	[OHBenz]	34.284
[HSO_4]	18.405	[F_3C1Benz]	29.563
[C_1SO_4]	18.344	[carzenide]	30.821
[C_2SO_4]	19.201	[PhBenz]	32.104
[C_4SO_4]	19.108	[BF_4]	2.487
[C_6SO_4]	19.051	[PF_6]	0.000
[$C_{12}SO_4$]	19.131	[H_2PO_4]	35.573
[$C_1OC_2SO_4$]	19.444	[DMP]	34.365
[$C_2OC_2SO_4$]	19.432	[DEP]	35.654
[TOS]	25.834	[DBP]	35.400
[TfO]	10.684	[F_6C_1B]	0.628
[DCN]	15.666	[$B(CN)_4$]	3.454
[TCN]	7.593	[$CH_2(CF_3SO_2)_2$]	3.419
[Benz]	32.252	[tf_2N]	1.974
[C_1Benz]	33.077	[$N(C_2F_6SO_2)_2$]	1.662
[C2Benz]	32.932	[$F_3P(C_2F_5)_3$]	0.019
[C_4Benz]	33.047	[$F_3P(C_3F_5)_3$]	0.041

The dissolution ability of ILs also increases with the increase in the hydrophobicity of anions (Fig. 10) which can also be observed from the sigma profile of the studied anions (Fig. S10). The peaks of the studied anions are mostly in the non polar range (Fig. S10). The first peak of the studied anions overlaps the peak of asphaltene molecule. The overlapping of sigma profiles of the hydrophobic anions with asphaltene molecule also indicates the dispersing ability of the present studied anions, i.e., $[F_3C_1Benz]^-$, $[CH_2(CF_3SO_2)_2]^-$, $[F_6C_1B]^-$ and $[NTF_2]^-$. The anions with increasing hydrophobicity (cations with longer alkyl chain length) show an increasing trend in the dispersing ability of ILs for asphaltene molecule.

Effect of alkyl chain length of anion. Different types of anions are considered to understand the impact of alkyl chain length of anion on the solubility of asphaltene molecule, i.e., [D C_n P] where n = 1, 2, 4, [C_n Benz] where n = 1,2 and 4, and [C_nSO_4] where n = 1,2,4,8 and 10. The estimated activity coefficient values of the present studied ILs are shown in Fig. 11 and Fig. S11 respectively. The solution capacity for asphaltene increases with the increase in the alkyl chain length of anion molecule (Fig. 11). Moreover, similar trends can be seen in other types of anions namely $[C_nBenz]^-$ and $[C_nSO_4]^-$, (Fig. S11). The magnitude of non polarity increases with the increase in the length of the alkyl tail in anion (Fig. S12). The overlapped peaks of the present studied anions, (Fig. S12), represent the polar characteristics of the functional group attached to the alkyl chain. The long alkyl chain of ILs helps in keeping the asphaltene molecule in dispersed form due to its steric stabilization effect [16]. It can be seen from the data on hydrogen bond acceptor and related energies, that the increase in alkyl chain length increases the hydrophobicity and Van der Waals interaction between the studied species and eventually responsible in increasing the solubility of asphaltene molecule. Similar trends of solubility and interaction energies can be observed for $[C_nBenz]^-$ and $[C_nSO_4]^-$ (Fig. S12) and Table 4 and 5, respectively.

Effect of the functional group of anions. The functional group alters the reactive ability of the anion. Therefore, various functional groups with similar head family are selected to understand the impact on the functional group of anions on the solubility of asphaltene using the estimated activity coefficient values. In the present study, various types of functional groups namely ether, hydroxyl, phenyl, and halide are investigated (Fig. 12). The order of solubility is as follows:

$$[OHBenz]^- < [ClBenz]^- < [Benz]^- < [C_1OBenz]^- < [PhBenz]^-$$

It is observed that the ether functionality slightly increases the interaction of the present studied IL with asphaltene molecule. However, solubility significantly increases with the addition of the phenyl group. The non polar region presented by the sigma profile of the studied ILs increases with the addition of the phenyl group which induces the hydrophobicity due to the Van der Waals interaction (Fig. S13). Consequently, the dispersive ability of the present studied ILs for asphaltene molecule increases. This can also be observed by the data on hydrogen bond acceptor of the studied anions as calculated by COSMO_RS (Table 4). In conclusion, the anion with higher hydrophobicity and stronger hydrogen bond energies has a higher affinity for asphaltene molecule and consequently higher dispersing strength. Furthermore, for the

Table 5
Misfit, Hydrogen bonding and Van der Waals energies for the capacity of asphaltene in the [C_6C_1im] based ILs at 298.15 K.

Anions	H^E_{MF} (kcal/mol)	H^E_{HB} (kcal/mol)	H^E_{vdW} (kcal/mol)	Anions	H^E_{MF} (kcal/mol)	H^E_{HB} (kcal/mol)	H^E_{vdW} (kcal/mol)
[Cl]	11.329	−1.87	−22.333	[FBenz]	8.817	−1.854	−21.664
[Br]	11.125	−1.665	−22.608	[ClBenz]	8.604	−1.826	−22.253
[I]	10.597	−1.456	−23.259	[BrBenz]	8.553	−1.827	−22.786
[Ac]	10.086	−2.209	−21.824	[IBenz]	8.509	−1.81	−23.34
[OHAc]	9.495	−1.886	−21.607	[C_1OBenz]	9.04	−1.822	−21.888
[TfAc]	8.681	−1.55	−20.656	[OHBenz]	8.655	−1.712	−21.832
[HSO_4]	9.588	−1.81	−21.464	[F_3C1Benz]	8.337	−1.765	−21.085
[C_1SO_4]	9.463	−1.447	−21.563	[carzenide]	8.464	−1.736	−21.77
[C_2SO_4]	9.21	−1.443	−21.549	[PhBenz]	8.642	−1.777	−22.108
[C_4SO_4]	9.27	−1.678	−21.579	[BF_4]	9.305	−1.317	−20.85
[C_6SO_4]	8.948	−1.643	−21.537	[PF_6]	8.446	−1.116	−20.112
[$C_{12}SO_4$]	7.892	−1.269	−21.401	[H_2PO_4]	9.793	−1.976	−21.515
[$C_1OC_2SO_4$]	9.19	−1.388	−21.458	[DMP]	9.606	−1.853	−21.712
[$C_2OC_2SO_4$]	8.918	−1.374	−21.45	[DEP]	9.147	−1.848	−21.633
[TOS]	9.034	−1.524	−21.82	[DBP]	8.609	−1.779	−21.548
[TfO]	8.352	−1.323	−20.452	[F_6C_1B]	8.147	−1.18	−19.99
[DCN]	9.112	−1.523	−21.826	[$B(CN)_4$]	8.061	−1.242	−21.781
[TCN]	8.479	−1.347	−21.851	[$CH_2(CF_3SO_2)_2$]	7.233	−1.179	−19.771
[Benz]	9.088	−1.884	−22.012	[tf_2N]	7.272	−1.131	−19.659
[C_1Benz]	8.991	−1.899	−21.971	[$N(C_2F_6SO_2)_2$]	6.949	−1.097	−19.142
[C2Benz]	8.813	−1.879	−21.935	[$F_3P(C_2F_5)_3$]	6.268	−1.154	−18.651
[C_4Benz]	8.559	−1.852	−21.878	[$F_3P(C_3F_5)_3$]	6.066	−1.117	−18.336

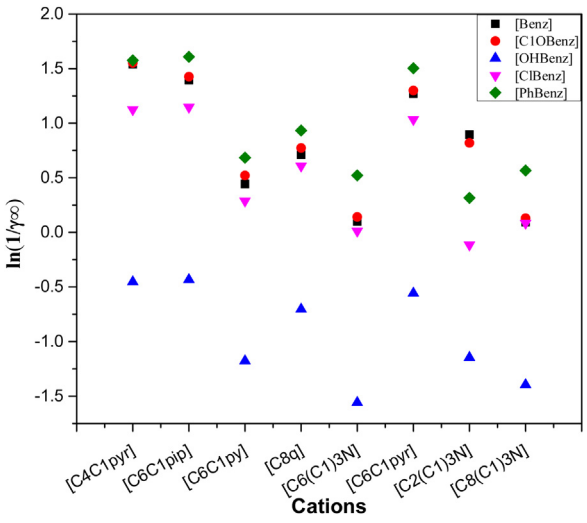

Fig. 12. Activity coefficient values of the studied ILs for asphaltene at 298.5 K.

same anion, the Van der Waals energy is higher when the alkyl chain is longer. Thus, the affinity for asphaltene molecule is stronger, and hence, the solubility is higher.

Conclusion

Due to the harmful environmental impact of traditional dispersants or solvents in dispersing aggregated asphaltene, using ILs as green dispersants for asphaltene aggregation problem in oil media are studied. In this work, the dispersive capability of 1517 potential ILs for asphaltene molecule was calculated using COSMO-RS. Following results, the impact of cation and anion family, their alkyl chain length and their functional group on the dispersive ability were investigated with the help of sigma profile, sigma moments, and hydrogen bond energies via COSMO-RS. It can be concluded that the dispersing ability of the ILs for asphaltene molecule depends on the nature of both cation and anion. The Van der Waals dispersion energies and Hydrogen bond donor-acceptor energies between ILs and asphaltene molecule significantly contribute to the solubility. The cations with long alkyl chain and hydrogen bond making ability have higher solubility with stronger Van der Waals energies and attraction. Similarly, the anion that has high hydrophobicity has a higher solubility for asphaltene with higher Van der Waals dispersion energies. The functional group attached to the anion also have an influence on the solubility of ILs. The functional group which increases the hydrophobicity and dispersion energies are suitable for dispersing of asphaltene molecule. The outcome of the present approach helps to understand the mechanism of asphaltene solubility and hence to develop targeted ILs for asphaltene dispersion in oil. Furthermore, it will open the doors to understand the solubility of species possessing complex molecular architectures such as polymers and metal organic frameworks by using ILs as dispersants.

Acknowledgment

This research is funded and facilitated by Centre of Research in Ionic liquids (CORIL), University Teknologi Petronas (UTP) Malaysia.

Appendix A. Supplementary data

Supplementary data associated with this article can be found, in the online version, at https://doi.org/10.1016/j.jiec.2019.06.034.

References

[1] S.-L. Chen, S.-S. Jia, Y.-H. Luo, S.-Q. Zhao, Fuel 73 (1994) 439.
[2] H. Alboudwarej, J. Beck, W.Y. Svrcek, H.W. Yarranton, K. Akbarzadeh, Energy Fuels 16 (2002) 462.
[3] P.E. Savage, M.T. Klein, Ind. Eng. Chem. Res. 27 (1988) 1348.
[4] I. Evdokimov, N. Eliseev, B. Akhmetov, Fuel 85 (2006) 1465.
[5] C.M. Smith, P.E. Savage, Ind. Eng. Chem. Res. 30 (1991) 331.
[6] D.L. Mitchell, J.G. Speight, Fuel 52 (1973) 149.
[7] S.I. Andersen, Energy Fuels 13 (1999) 315.
[8] S. Gharfeh, A. Yen, S. Asomaning, D. Blumer, Petrol. Sci. Technol. 22 (2004) 1055.
[9] F. Mutelet, G. Ekulu, R. Solimando, M. Rogalski, Energy Fuels 18 (2004) 667.
[10] L. Goual, J.F. Schabron, T.F. Turner, B.F. Towler, Energy Fuels 22 (2008) 4019.
[11] S.I. Andersen, S.D. Christensen, Energy Fuels 14 (2000) 38.
[12] J.H. Pacheco-Sánchez, I.P. Zaragoza, J.M. Martínez-Magadán, Energy Fuels 17 (2003) 1346.
[13] J.A. Koots, J.G. Speight, Fuel 54 (1975) 179.
[14] Y.-F. Hu, T.-M. Guo, Langmuir 21 (2005) 8168.
[15] C.-L. Chang, H. Scott Fogler, Fuel Sci. Technol. Int. 14 (2007) 75.
[16] M. Boukherissa, F. Mutelet, A. Modarressi, A. Dicko, D. Dafri, M. Rogalski, Energy Fuels 23 (2009) 2557.
[17] H.-f. Fan, Z.-b. Li, T. Liang, J. Fuel Chem. Technol. 35 (2007) 32.
[18] Y. Zhou, N. Xiao, J. Qiu, Y. Sun, T. Sun, Z. Zhao, Y. Zhang, N. Tsubaki, Fuel 87 (2008) 3474.
[19] Z.-x. Fan, T.-f. Wang, Y.-h. He, J. Fuel Chem. Technol. 37 (2009) 690.
[20] J. Li, J. Yang, Z. Liu, Fuel Process. Technol. 90 (2009) 490.
[21] Y. Li, X. Zhang, H. Dong, X. Wang, Y. Nie, S. Zhang, RSC Adv. 1 (2011).
[22] Y. Nie, L. Bai, Y. Li, H. Dong, X. Zhang, S. Zhang, Ind. Eng. Chem. Res. 50 (2011) 10278.
[23] E. Rezaee Nezhad, F. Heidarizadeh, S. Sajjadifar, Z. Abbasi, J. Petrol. Eng. (2013) (2013) 1.
[24] A.S. Ogunlaja, E. Hosten, Z.R. Tshentu, Ind. Eng. Chem. Res. 53 (2014) 18390.
[25] Z. Rashid, C.D. Wilfred, N. Gnanasundaram, A. Arunagiri, T. Murugesan, J. Mol. Liq. 255 (2018) 492.
[26] M. Kar, N.V. Plechkova, K.R. Seddon, J.M. Pringle, D.R. MacFarlane, Aust. J. Chem. 72 (2019) 3.
[27] N. Calvar, I. Domínguez, E. Gómez, J. Palomar, Á. Domínguez, J. Chem. Thermodyn. 67 (2013) 5.
[28] N. Muhammad, G. Gonfa, A. Rahim, P. Ahmad, F. Iqbal, F. Sharif, A.S. Khan, F.U. Khan, Z.U.L.H. Khan, F. Rehman, I.U. Rehman, J. Mol. Liq. 232 (2017) 258.
[29] A. Klamt, J. Phys. Chem. 99 (1995) 2224.
[30] A. Klamt, F. Eckert, Fluid Phase Equilib. 172 (2000) 43.
[31] A. Klamt, V. Jonas, T. Bürger, J.C.W. Lohrenz, J. Phys. Chem. A 102 (1998) 5074.
[32] M. Hornig, A. Klamt, J. Chem. Inf. Model. 45 (2005) 1169.
[33] A. Klamt, G. Schüürmann, J. Chem. Soc., Perkin Trans. 2 (1993) 799.
[34] J. Andzelm, C. Kölmel, A. Klamt, J. Chem. Phys. 103 (1995) 9312.
[35] A. Klamt, F. Eckert, W. Arlt, Annu. Rev. Chem. Biomol. Eng. 1 (2010) 101.
[36] K.N. Marsh, J. Chem. Eng. Data 51 (2006) 1480.
[37] F. Eckert, A. Klamt, Ind. Eng. Chem. Res. 40 (2001) 2371.
[38] M. Fermeglia, S. Pricl, AIChE J. 47 (2001) 2371.
[39] S.-T. Lin, S.I. Sandler, Ind. Eng. Chem. Res. 41 (2002) 899.
[40] R. Putnam, R. Taylor, A. Klamt, F. Eckert, M. Schiller, Ind. Eng. Chem. Res. 42 (2003) 3635.
[41] A. Klamt, F. Eckert, M. Hornig, M.E. Beck, T. Burger, J. Comput. Chem. 23 (2002) 275.
[42] A. Klamt, Fluid Phase Equilib. 206 (2003) 223.
[43] K. Kędra-Kro'lik, M. Fabrice, J.-Nl. Jaubert, Ind. Eng. Chem. Res. 50 (2011) 2296.
[44] R. Anantharaj, T. Banerjee, Ind. Eng. Chem. Res. 49 (2010) 8705.
[45] Y. Li, L.-S. Wang, Y.-X. Feng, C.-Y. Zhang, Ind. Eng. Chem. Res. 50 (2011) 10755.
[46] C. Jork, C. Kristen, D. Pieraccini, A. Stark, C. Chiappe, Y.A. Beste, W. Arlt, J. Chem. Thermodyn. 37 (2005) 537.
[47] M. Thormann, A. Klamt, M. Hornig, M. Almstetter, J. Chem. Inf. Model. 46 (2006) 1040.
[48] T. Kuznicki, J.H. Masliyah, S. Bhattacharjee, Energy Fuels 22 (2008) 2379.
[49] J.H. Pacheco-Sánchez, F. Álvarez-Ramírez, J.M. Martínez-Magadán, Energy Fuels 18 (2004) 1676.
[50] D. Pradilla, S. Simon, J. Sjoblom, J. Samaniuk, M. Skrzypiec, J. Vermant, Langmuir 32 (2016) 2900.
[51] J. Sjoblom, S. Simon, Z. Xu, Adv. Colloid Interface Sci. 218 (2015) 1.
[52] E.Lk. Nordgård, J. Sjöblom, J. Disper. Sci. Technol. 29 (2008) 1114.
[53] A. Schäfer, A. Klamt, D. Sattel, J.C.W. Lohrenz, F. Eckert, Phys. Chem. Chem. Phys. 2 (2000) 2187.
[54] M. Lotfi, M. Moniruzzaman, M. Sivapragasam, S. Kandasamy, M.I. Abdul Mutalib, N.B. Alitheen, M. Goto, J. Mol. Liq. 243 (2017) 124.
[55] T. Zhou, L. Chen, Y. Ye, L. Chen, Z. Qi, H. Freund, K. Sundmacher, Ind. Eng. Chem. Res. 51 (2012) 6256.
[56] H. Wang, C. Xie, S. Yu, F. Liu, Chem. Eng. J. 237 (2014) 286.
[57] S. Gao, X. Chen, R. Abro, A.A. Abdeltawab, S.S. Al-Deyab, G. Yu, Ind. Eng. Chem. Res. 54 (2015) 9421.
[58] R. Anantharaj, T. Banerjee, Fuel Process. Technol. 92 (2011) 39.
[59] C.C. Brunchi, P. Englebienne, H.J.M. Kramer, S.K. Schnell, T.J.H. Vlugt, Mol. Simulat. 41 (2015) 1234.
[60] P. Matheswaran, C.D. Wilfred, K.A. Kurnia, A. Ramli, Ind. Eng. Chem. Res. 55 (2016) 788.

[61] S. Rezaei Motlagh, R. Harun, D.R. Awang Biak, S.A. Hussain, W.A. Wan Ab Karim Ghani, R. Khezri, C.D. Wilfred, A.A.M. Elgharbawy, Molecules 24 (2019) 713.
[62] A. Heintz, D.V. Kulikov, S.P. Verevkin, J. Chem. Eng. Data 47 (2002) 894.
[63] C. Loschen, A. Klamt, J. Pharm. Pharmacol. 67 (2015) 803.
[64] S. Oleszek-Kudlak, M. Grabda, E. Shibata, F. Eckert, T. Nakamurat, Environ. Toxicol. Chem. 24 (2005) 1368.
[65] M. Diedenhofen, A. Klamt, Fluid Phase Equilib. 294 (2010) 31.
[66] J. Kahlen, K. Masuch, K. Leonhard, Green Chem. 12 (2010).
[67] A. Casas, J. Palomar, M.V. Alonso, M. Oliet, S. Omar, F. Rodriguez, Ind. Crops Prod. 37 (2012) 155.
[68] G. Gonfa, N. Muhammad, M. Azmi Bustam, Sep. Purif. Technol. 196 (2018) 237.
[69] M. Agrawala, H.W. Yarranton, Ind. Eng. Chem. Res. 40 (2001) 4664.
[70] V.A.M. Branco, G.A. Mansoori, L.C. De Almeida Xavier, S.J. Park, H. Manafi, J. Petrol. Sci. Eng. 32 (2001) 217.
[71] J. Murgich, Mol. Simulat. 29 (2003) 451.
[72] M. Królikowska, M. Karpińska, Fluid Phase Equilib. 400 (2015) 1.
[73] A. Navas, J. Ortega, T. Martín, J. Palomar, Ind. Eng. Chem. Res. 49 (2010) 12726.
[74] Z. Rashid, C.D. Wilfredand, T. Murugesan, Effect of Hydrophobic Ionic Liquids on Petroleum Asphaltene Dispersion and Determination Using UV-visible Spectroscopy, (2017) .
[75] C.C. Cassol, A.P. Umpierre, G. Ebeling, B. Ferrera, S.S.X. Chiaro, J. Dupont, Int. J. Mol. Sci. 8 (2007) 593.
[76] R. Anantharaj, T. Banerjee, Fluid Phase Equilib. 293 (2010) 22.
[77] K.A. Kurnia, F. Lima, A.F.M. Cláudio, J.A.P. Coutinho, M.G. Freire, Phys. Chem. Chem. Phys. 17 (2015) 18980.
[78] H.F. Hizaddin, M.A. Hashim, R. Anantharaj, Ind. Eng. Chem. Res. 52 (2013) 18043.
[79] M.G. Freire, C.M.S.S. Neves, K. Shimizu, C.E.S. Bernardes, I.M. Marrucho, J.A.P. Coutinho, J.N.C. Lopes, L.P.N. Rebelo, J. Phys. Chem. B 114 (2010) 15925.
[80] M.G. Freire, C.M.S.S. Neves, S.P.M. Ventura, M.J. Pratas, I.M. Marrucho, J. Oliveira, J.A.P. Coutinho, A.M. Fernandes, Fluid Phase Equilib. 294 (2010) 234.
[81] J. Wang, N. van der Tuuk Opedal, Q. Lu, Z. Xu, H. Zeng, J. Sjöblom, Energy Fuels 26 (2011) 2591.
[82] P. Wiwel, K. Knudsen, P. Zeuthen, D. Whitehurst, Ind. Eng. Chem. Res. 39 (2000) 533–540.